International Journal of Heat and Technology
Vol. 42, No. 6, December, 2024, pp. 2185-2192
Journal homepage: http://iieta.org/journals/ijht

Optimization of Office Ventilation Strategies Using the FLUENT Component Transport Model: A Numerical Simulation Approach

Bin Zhang[1*], Yin Liu[2], Shaoxiong Zhang[2]

[1] Hebei Chemical & Pharmaceutical College, Shijiazhuang 050000, China
[2] College of Civil Engineering, Shijiazhuang Tiedao University, Shijiazhuang 050043, China

Corresponding Author Email: 271920018@qq.com

https://doi.org/10.18280/ijht.420637

Received: 19 July 2024
Revised: 8 October 2024
Accepted: 2 November 2024
Available online: 31 December 2024

Keywords:
volatile organic compounds, FLUENT, component transport, numerical simulation

ABSTRACT

In modern society, a significant proportion of time is spent indoors, where exposure to volatile organic compounds (VOCs) emitted by various office equipment and materials is common. These harmful gases can cause irreversible health damage upon inhalation. Therefore, reducing the concentration of indoor VOCs has become a topic of great concern. Selecting an appropriate ventilation strategy is an effective and practical method to lower pollutant concentrations. In this study, a typical office and its ventilation system were numerically simulated using the standard k-ε turbulence model and the component transport model in FLUENT. Four scenarios with different inlet airflow velocities and three scenarios with varying inlet airflow angles were evaluated. The concentrations and distributions of VOCs were analyzed at both seated and standing breathing planes as well as within the overall space. It was observed that higher inlet airflow velocities, within the limits of human comfort, accelerated indoor air exchange, reaching dynamic equilibrium more swiftly. Additionally, both the breathing zone and the indoor space exhibit lower average concentrations of VOCs after equilibrium was achieved as the inlet velocity increased. Furthermore, under a constant inlet velocity, an upward 45° airflow angle was found to create more effective indoor air mixing, reduce stagnant zones, and facilitate VOC removal, thereby lowering indoor VOC concentrations. Based on the findings, a ventilation strategy employing a larger inlet airflow velocity combined with an upward airflow angle is recommended to efficiently reduce indoor VOC concentrations, improve air quality, and mitigate health risks. These results provide valuable guidance for the design and implementation of ventilation systems in real-world engineering applications.

1. INTRODUCTION

With the rapid advancement of societal development and urbanization, the proportion of time spent indoors has significantly increased. However, during interior decoration, the use of materials containing VOCs is often unavoidable, resulting in concerns regarding indoor air quality. According to national standards for the coatings industry, VOCs are defined as any organic liquids and/or solids that can naturally evaporate under normal atmospheric temperature and pressure [1]. In typical office environments, the primary sources of VOC emissions include coatings such as wood varnishes used on desks and chairs. These compounds are released from the coatings into the indoor air, where they can be inhaled by occupants.

On average, individuals spend approximately 90% of their time indoors, with the duration being even higher for vulnerable populations such as the elderly and children. Consequently, the quality of indoor air is closely linked to human health [2]. VOCs contain substances that pose significant health risks, including benzene, formaldehyde, and other well-known harmful compounds, many of which exhibit strong carcinogenicity and toxicity [3-5]. According to the World Health Organization (WHO), indoor air pollution has been implicated in 36% of respiratory diseases, 22% of chronic lung diseases, and 15% of tracheitis and bronchitis cases [6].

Mitigating the harmful effects of VOCs has become a matter of increasing concern. Current methods for VOC degradation include persulfate oxidation [7], titanium dioxide (TiO_2) photocatalytic degradation [8], and adsorption using engineered carbon materials [9]. However, these approaches primarily focus on source control and pollutant treatment. In everyday life, the most convenient and effective method for reducing indoor VOC concentrations involves improving ventilation, thereby reducing the concentration of VOCs indoors.

In studies addressing the improvement of indoor air quality through ventilation, Computational Fluid Dynamics (CFD) techniques are primarily utilized for numerical simulations. These simulations generate airflow streamlines, wind velocities at various locations, and concentrations of VOCs, among other parameters. Such data enables the determination of pollutant concentration distributions and variation patterns under different ventilation methods, thereby providing theoretical support and guidance for the selection of

appropriate ventilation strategies.

Numerous studies have been conducted by research institutions and experts on VOC emissions and ventilation. Hun et al. [10] investigated 179 residential buildings in the United States and identified a strong correlation between the total volatile organic compound (TVOC) concentrations and factors such as building design, construction age, frequency of indoor-outdoor air exchange, indoor temperature, and seasonal variations. Yang and Chen [11] employed the Reynolds-averaged Navier-Stokes equations and the RNG k-ε vortex viscosity turbulence model to numerically simulate the distribution of indoor pollutant concentrations and the effectiveness of pollutant removal under different ventilation strategies, providing theoretical guidance for optimizing ventilation designs. Sun et al. [12] utilized direct numerical simulation (DNS) techniques to calculate indoor ventilation flow fields, describing airflow evolution and vortex structures within indoor environments. Verniers et al. [13] discussed in-situ indoor measurements of PM and VOCs caused by cooking, vacuuming, and burning candles under different ventilation options, emphasizing the importance of creating healthy indoor spaces by reducing air pollutants and ensuring comfort. Zemitis et al. [14] analyzes VOC concentration changes from various sources in both closed and ventilated environments, revealing three distinct dynamics, and suggests that post-painting, hazardous VOC levels may persist for 12 hours under regulated ventilation, with data aiding future studies, prediction methods, and ventilation standards. Yan et al. [15] simulated velocity and temperature fields under natural ventilation conditions for two residential layouts using FLUENT, recommending optimal ventilation layouts based on the findings. Lee and Awbi [16] combined numerical simulations with experiments to investigate how the placement of pollution sources and spatial configurations in an upward airflow mode affected pollutant concentration distributions and ventilation efficiency. Pereira et al. [17] used model experiments to analyze the effects of four ventilation strategies on indoor pollutant distributions. Visagavel and Srinivasan [18] simulated fresh air flow rates for two ventilation schemes using FLUENT, concluding that increasing window height could enhance cross-ventilation efficiency. Cheong et al. [19] integrated numerical simulations with experimental data to study pollutant distributions in an office model with planar pollution sources. Ye et al. [20] introduced two new methods—the characteristic ventilation rate method and the two-stage ventilation rate method—for predicting ventilation rates based on building material emissions, revealing that ventilation rates vary with reference standards, materials, emission areas, and can be reduced by half with steady-state rates due to the overestimation tendency of the characteristic method, with complete emission periods spanning 2.5 to 5 years. Hernandez et al. [21] investigated the impact of airtightness and ventilation on VOC concentrations in newly-furnished unoccupied houses and controlled simulated occupancy rooms, revealing that airtightness delays the peak VOC concentration and slows decay, while mechanical ventilation significantly reduces TVOC levels but may not suffice to protect occupants from prolonged exposure after chemical use. Kang et al. [22] investigated the VOC emission and sorption characteristics of adhesive-bonded materials in a radiant floor heating system, focusing on emission-dominated (e.g., plywood/epoxy) and sorption-dominated (e.g., PVC wallpaper/starch-based adhesive/gypsum board) materials, using numerical analysis validated by experimental data, and discussing the impact on indoor air quality. Xiao et al. [23] studied the adsorption of VOCs on a new swirling fluidized bed through numerical simulation and experiments, expanding its application in VOC removal, and found optimal conditions for maximum adsorption efficiency with minimal activated carbon damage. Liu and Li [24] investigated a long-term numerical study on airflow patterns, benzene VOC distribution, and a ventilation strategy in a typical apartment building in China's severe cold region. Song et al. [25] established an analytical model to investigate VOC emission from wood furniture, enabling the prediction of mass transfer characteristics and proposing a rapid experimental method to determine key mass transfer parameters.

In this study, the standard k-ε turbulence model and component transport model in FLUENT were employed to simulate air conditioning ventilation schemes in a typical office. The effects of inlet airflow velocity and angle on reducing VOC concentrations were explored. Reasonable ventilation strategies were analyzed and proposed to provide reference guidance for the design of ventilation layouts.

2. BASIC THEORY

2.1 Mass conservation equation

Mass conservation refers to the rate of change in the mass of fluid within a control volume, which is equal to the net mass flux into the volume over a given time interval. The equation is expressed as:

$$\frac{\partial \rho}{\partial t} + \frac{\partial}{\partial x_i}(\rho u_i) = S_m \tag{1}$$

where, ρ is the airflow density, u_i is the airflow velocity, with the subscripts i=1,2,3 corresponding to the x, y, and z directions, respectively, and S_m is the source term.

In indoor fluids, air can be treated as an incompressible gas; thus, the continuity equation can be simplified to:

$$\frac{\partial u_i}{\partial x_i} = 0 \tag{2}$$

2.2 Momentum conservation equation

Momentum conservation refers to the rate of change in momentum of the fluid within a control volume, which is equal to the sum of the external forces acting on that volume. The expression is given by:

$$\frac{\partial}{\partial_t}(\rho u_i) + \frac{\partial}{\partial_{x_j}}(\rho u_i u_j) = -\frac{\partial p}{\partial_{x_i}} + \frac{\partial \tau_{ij}}{\partial_{x_j}} + \rho g_i + F_i \tag{3}$$

where, p is the static pressure, τ_{ij} is the stress tensor, g_i is the gravitational body force in the i-th direction, and F_i is the external body force in the i-th direction.

2.3 Component equation

In a system with multiple chemical components, each component must satisfy the mass conservation law. In this study, a component transport model without chemical

reactions was employed. The component mass conservation equation for component s is expressed as:

$$\frac{\partial(\rho c_s)}{\partial t} + \frac{\partial}{\partial x_i}(\rho u_i c_s) = \frac{\partial}{\partial x_j}(\rho D_s \frac{\partial c_s}{\partial x_j}) \quad (4)$$

where, c_s is the volume concentration of component s; ρc_s is the mass concentration of component s; and D_s is the diffusion coefficient of component s.

2.4 Turbulence control equations

The equation for turbulence kinetic energy k is given by:

$$\rho \frac{\partial k}{\partial t} = \frac{\partial}{\partial x_i}\left[\left(\mu + \frac{\mu_t}{\sigma_k}\right)\frac{\partial k}{\partial x_i}\right] + G_k + G_b - \rho\varepsilon - Y_M \quad (5)$$

The equation for turbulence dissipation rate ε is given by:

$$\rho \frac{\partial \varepsilon}{\partial t} = \frac{\partial}{\partial x_i}\left[\left(\mu + \frac{\mu_t}{\sigma_\varepsilon}\right)\frac{\partial \varepsilon}{\partial x_i}\right] + C_{1\varepsilon}\frac{\varepsilon}{k}(G_k + G_{3b}G_b) - C_{2\varepsilon}\rho\frac{\varepsilon^2}{k} \quad (6)$$

where, G_k is the production of turbulent kinetic energy due to the mean velocity gradient, G_b is the production of turbulent kinetic energy due to buoyancy, and Y_M is the effect of compressible turbulent fluctuations on the total dissipation rate.

2.5 VOC mass fraction and concentration conversion equation

$$c_{VOCs} = \frac{m_{VOCs}}{V_a} = \frac{m_{VOCs}}{V_a \cdot \rho_a} \times \rho_a = \frac{m_{VOCs}}{m_a} \times \rho_a = w_{VOCs} \cdot \rho_a \times 10^6 \quad (7)$$

where, c is the VOC concentration (mg/m³); m_{VOCs} is the mass of VOCs (mg); V_a is the volume of air (m³); P_a is the density of air (kg/m³); m_a is the mass of air (kg); and w_{VOCs} is the mass fraction of VOCs.

3. MODEL DEVELOPMENT

A common office was selected as the model for the simulation and the model was simplified for the purpose of analysis. The indoor dimensions of the office were 6.45 m × 5.6 m × 2.85 m. A 0.4 m × 0.25 m air conditioning inlet was placed 1.5 m above the ground as the air intake. A 1.95 m × 0.85 m door was positioned diagonally opposite the air intake as the exhaust outlet. A 1 m × 1 m × 1 m cube was placed at the center of the office floor as the pollution source, emitting pollutants from five surfaces. The x-axis was aligned with the width, the y-axis with the length, and the z-axis was oriented vertically upwards. The geometric model is shown in Figure 1(a), and the mesh division is shown in Figure 1(b).

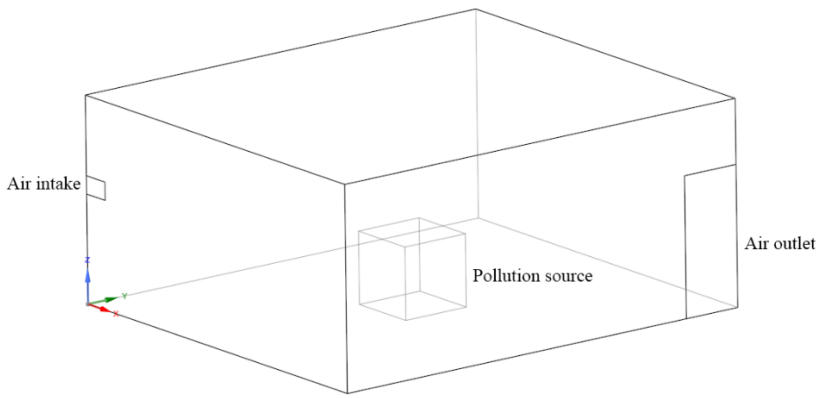

(a) Geometric model

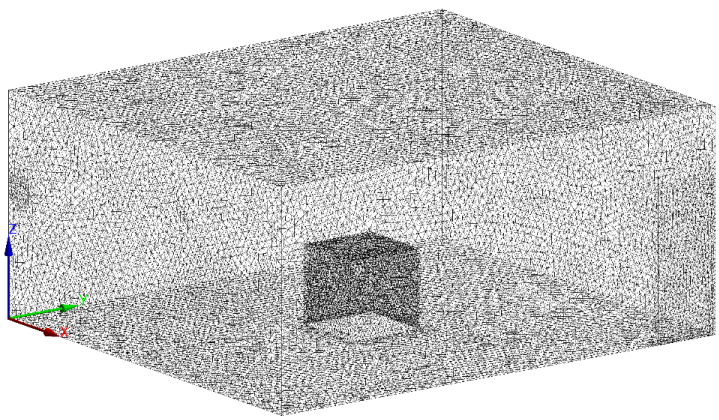

(b) Mesh division

Figure 1. Geometric model and mesh division

Boundary conditions: The initial VOC concentration indoors was set to 0. The air intake consisted of air with a VOC content of 0. The inlet boundary condition was defined as a velocity inlet. The pollution source of VOCs was modeled as a mass flow inlet, with a constant release rate of 7.2e-11 kg/s. The air outlet was simplified as a pressure outlet. The office walls were treated as adiabatic boundaries, and radiation heat transfer was neglected.

4. NUMERICAL SIMULATION AND ANALYSIS

Several factors influence the effectiveness of ventilation, including the position, quantity, specifications, and type of the air intakes and outlets; the inlet air velocity and angle of incidence; the indoor air temperature and humidity; as well as the room shape. This study focuses on the effects of two key factors on ventilation effectiveness: the inlet airflow velocity and the angle of incidence of the air intake on the indoor VOC concentration field. Initially, the impact of varying air velocities on pollutant concentration distribution was considered when the angle of incidence was fixed (45° relative to the horizontal plane and vertical wall, maintaining a horizontal angle in the vertical plane), which corresponds to operating conditions 1, 2, 3, and 4. Subsequently, under the optimal wind velocity, the horizontal angle was maintained while the vertical inlet angle was varied, representing operating conditions 5 and 6, as illustrated in Figure 2.

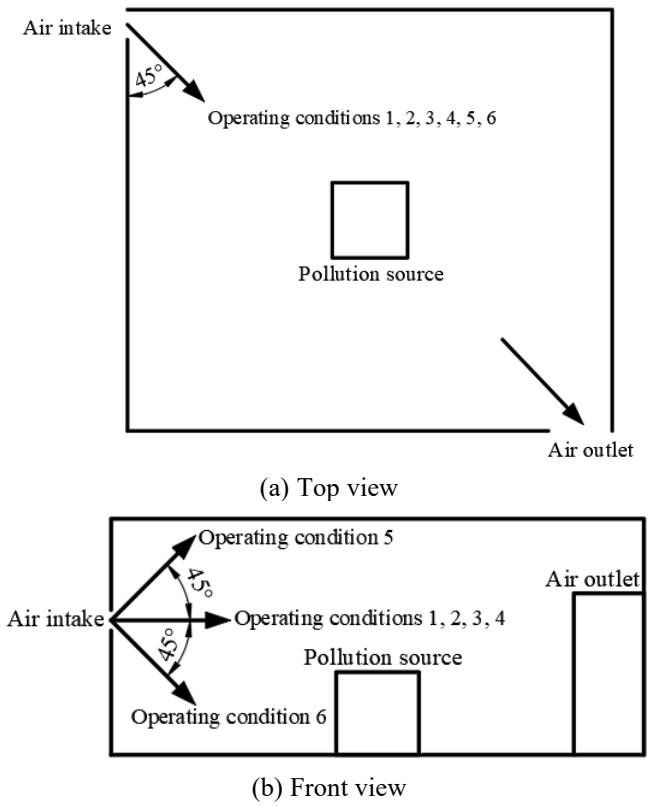

Figure 2. Schematic diagram of inlet airflow angles for different operating conditions

The VOC mass fraction distribution contour maps at the z=1.2 m plane (representing the breathing height while seated) and the z=1.5 m plane (representing the breathing height while standing) were extracted and the average VOC mass fractions at the corresponding planes were monitored in order to reflect the pollutant concentration distribution in the two-dimensional horizontal plane. Additionally, the average VOC mass fraction across the entire flow field was monitored to represent the pollutant concentration in three-dimensional space, thus indicating the potential harm of VOCs to human health. This data was used to compare various ventilation methods, with the most effective ventilation strategy being identified.

4.1 Simulation and analysis of different inlet airflow velocities

The effect of different air velocities on the pollutant concentration was first studied, assuming a fixed incident angle. Considering that the air velocity from air conditioning systems should not cause discomfort to the human body, the air velocity was not set to excessively high values. Air velocities of 1 m/s, 1.5 m/s, 2 m/s, and 2.5 m/s were selected for the simulations. The VOC mass fraction distribution during 3600 seconds of ventilation was calculated for each air velocity, corresponding to operating conditions 1, 2, 3, and 4. The results are presented in Figures 3 and 4. The average VOC mass fractions for both planes under each air velocity were calculated and provided in Table 1. The variation of the spatial average VOC mass fraction with time is shown in Figure 5.

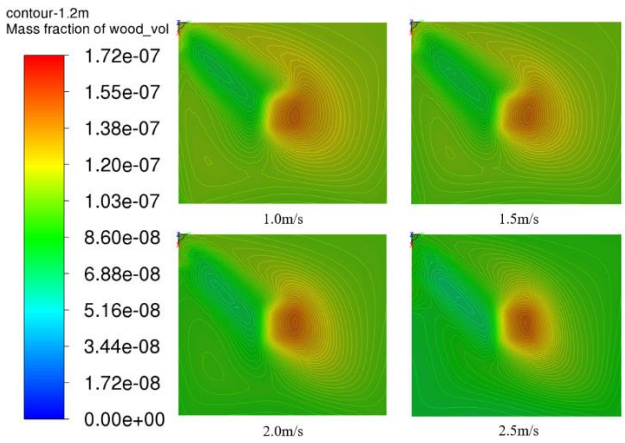

Figure 3. Distribution of VOC mass fractions at the z = 1.2 m plane for different inlet airflow velocities

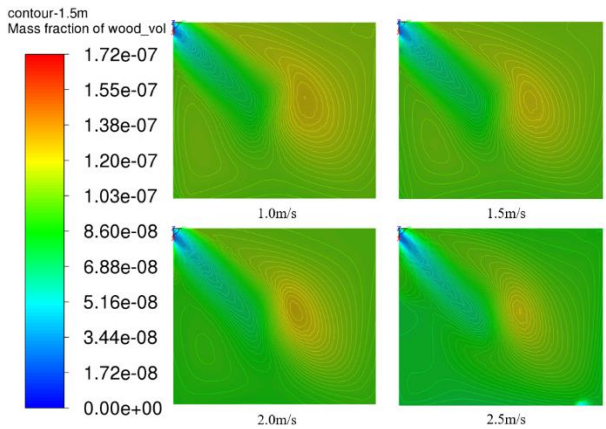

Figure 4. Distribution of VOC mass fractions at the z = 1.5 m plane for different inlet airflow velocities

It can be observed from Figures 3 and 4 that fresh air is introduced horizontally through the inlet into the office space. As it passes the location of the pollution source, VOCs are

carried along by the airflow. Upon encountering the walls, the direction of airflow is altered, leading to the formation of a vortex zone. Ultimately, the air exits through the outlet. This process results in a lower VOC mass fraction near the inlet and a higher VOC mass fraction near the pollution source. The formation of the vortex zone leads to the creation of "dead zones" at the lower left and upper right corners, where the VOC mass fraction is elevated. Comparing the VOC mass fraction distribution diagrams at different wind velocities, as well as referring to Table 1, it can be noted that the VOC mass fraction at the z = 1.2 m plane is always higher than that at the z = 1.5 m plane. This is due to the proximity of the z = 1.2 m plane to the pollution source. Regardless of the plane, whether at z = 1.2 m or z = 1.5 m, the average VOC mass fraction decreases as the wind velocity increases.

Table 1. Average VOC mass fractions at different planes for various inlet airflow velocities

	v = 1.0 m/s	v = 1.5 m/s	v = 2.0 m/s	v = 2.5 m/s
z =1.2 m	1.10e-07	1.07e-07	1.02e-07	9.45e-08
z =1.5 m	1.01e-07	9.75e-08	9.35e-08	8.60e-08

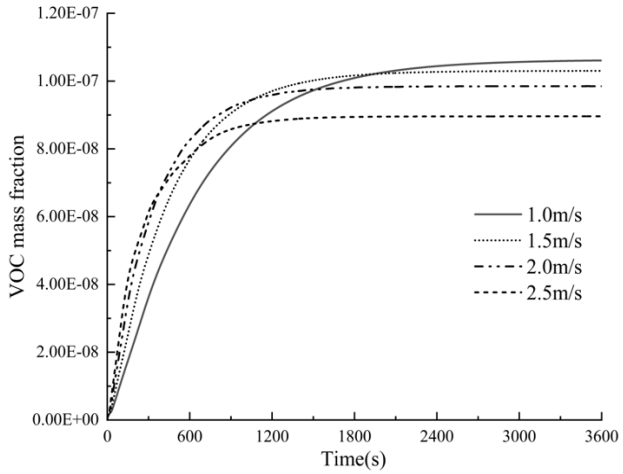

Figure 5. Variation of spatial average VOC mass fraction over time

From Figure 5, it can be observed that the trends in the variation of spatial VOC mass fraction over time are consistent across different inlet airflow velocities. Initially, the VOC mass fraction increases with time, as an insufficient amount of fresh air enters the room to expel the pollutants through the outlet. After a certain period of ventilation, the pollutant mass fraction tends to stabilize, signifying that a dynamic equilibrium state has been reached in the airflow within the room. It can be seen from the figure that curves corresponding to higher wind velocities reach the inflection point of the curve earlier and achieve a lower stable value. This indicates that, with higher wind velocities, the airflow within the space reaches dynamic equilibrium more quickly, and the VOC concentration within the space is reduced to a lower level.

An analysis combining both two-dimensional plane and three-dimensional spatial perspectives reveals that higher inlet airflow velocities result in lower VOC concentrations within the room, thereby improving the ventilation effectiveness.

4.2 Simulation and analysis of different inlet airflow angles

Under the optimal ventilation wind velocity condition (2.5 m/s), simulations were conducted to investigate the impact of different inlet angles on the indoor VOC concentration distribution. The inlet angle was fixed at 45° in the horizontal plane, while in the vertical plane, it was set to horizontal, 45° upward, and 45° downward (as shown in Figure 2), i.e., operating conditions 4, 5 and 6. The resulting VOC relative mass fraction distribution at 3600 s is depicted in Figures 6 and 7, and the streamlines are shown in Figure 8. The average VOC mass fractions for the two planes at each wind speed were calculated and are presented in Table 2. The variation of spatial VOC average mass fraction over time is illustrated in Figure 9.

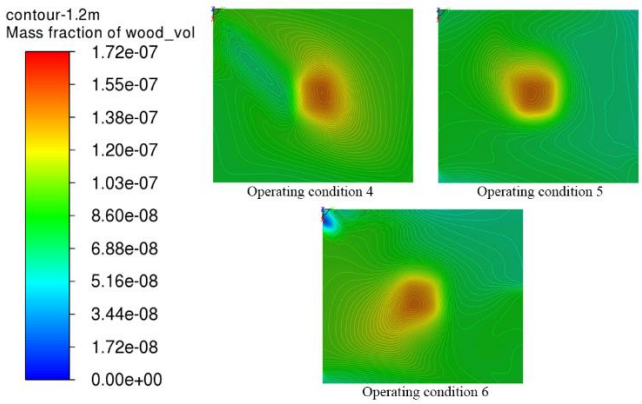

Figure 6. Distribution of VOC mass fractions at the 1.2 m plane

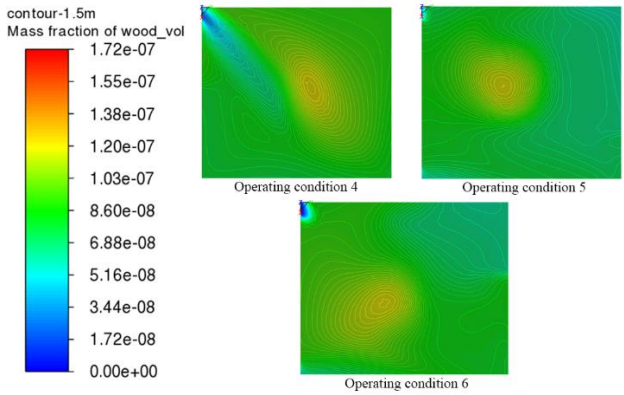

Figure 7. Distribution of VOC mass fractions at the 1.5 m plane

Table 2. Average VOC mass fractions at different inlet airflow angles

	Operating Condition 4: Horizontal	Operating Condition 5: Upward 45°	Operating Condition 6: Downward 45°
z = 1.2 m	9.45e-08	8.43e-08	8.89e-08
z = 1.5 m	8.60e-08	7.77e-08	8.36e-08

It can be observed from the plane distribution cloud maps that when fresh air enters the room at different angles, the VOC mass fraction near the inlet is lower, while the VOC mass fraction near the pollutant source is higher. The varying angles of inflow lead to different levels of disturbance in the indoor air, which results in changes in the locations and areas of the "dead zones" of pollutants within the plane. The VOC

mass fraction in the plane of operating condition 4 is generally higher than in conditions 5 and 6, while the "dead zone" area in operating condition 5 is smaller than in operating condition 6. Based on the data in Table 2, it can be concluded that the VOC mass fraction at the z = 1.2 m plane is greater than at the z = 1.5 m plane for all conditions, primarily due to the proximity of the z = 1.2 m plane to the pollutant source. The average VOC mass fractions at both the z = 1.2 m and z = 1.5 m planes follow the order of operating condition 4 > operating condition 6 > operating condition 5.

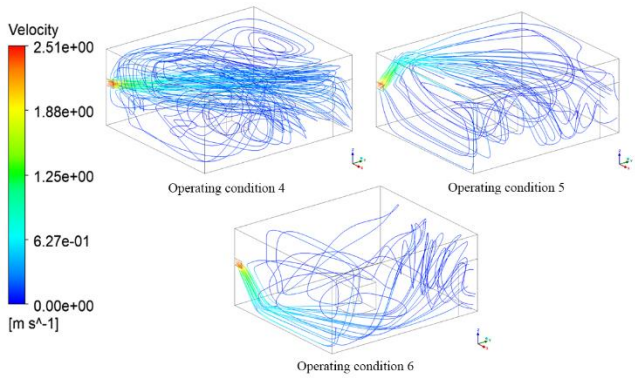

Figure 8. Streamlines for different inlet airflow angles

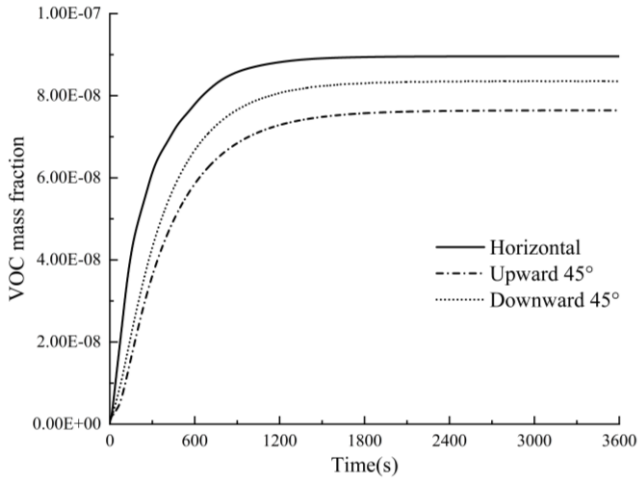

Figure 9. Variation of the average VOC mass fraction in space over time

From the streamline diagram (Figure 8) and the curve graph (Figure 9), it can be observed that in operating condition 4, with horizontal inflow, when the airflow contacts the wall, a boundary layer flow is formed along the wall, gradually reducing in velocity, resulting in longer streamlines. The vortex zone created by the airflow recirculation is larger, which increases the residence time of the gas within the space. The airflow mainly disturbs the upper portion of the room, with minimal disturbance to the lower half. Due to the higher density of VOCs compared to air, the pollutants tend to deposit in the lower part of the space, preventing them from being effectively expelled through the outlet, leading to a higher average VOC mass fraction in the space. In operating condition 5, with an upward 45° inflow, the disturbance to the air in both the upper and lower directions is more significant, allowing the airflow to carry the pollutants more efficiently to the outlet, thereby reducing the average VOC mass fraction in the space. In operating condition 6, with a downward 45° inflow, although similar to condition 5, there is a better disturbance to the VOCs that are deposited in the lower portion of the room; the location of the pollution source obstructs the movement of the air, resulting in a large "dead zone" on the leeward side of the source. This accumulation of pollutants contributes to a higher average VOC mass fraction in the space for this condition. As can be clearly seen in Figure 9, although the time for the curves to reach the inflection point is similar for all three conditions, the dynamic equilibrium is reached at the lowest average VOC mass fraction in condition 5.

A comprehensive analysis of both the two-dimensional plane and three-dimensional space reveals that, in terms of reducing VOC concentrations, the upward 45° inflow is more effective than the downward 45° inflow, and the downward 45° inflow is more effective than the horizontal inflow in the operating conditions with three different inlet airflow angles.

4.3 Conversion of simulation results

The average VOC mass fractions for the planes and the space of each operating condition were converted into VOC concentrations using Eq. (7). This conversion allowed for the determination of whether the results of each operating condition complied with the VOC concentration limit of 0.60 mg/m³, as specified by *the Indoor Air Quality Standard (GB/T 18883-2022)* [26]. The results are shown in Table 3.

Table 3. Conversion of simulation results

Operating Condition	Location	Mass Fraction	Concentration (mg/m³)
Condition 1	z=1.2m	1.10e-07	0.130
	z=1.5m	1.01e-07	0.120
	Indoor space	1.06e-07	0.126
Condition 2	z=1.2m	1.07e-07	0.127
	z=1.5m	9.75e-08	0.116
	Indoor space	1.03e-07	0.122
Condition 3	z=1.2m	1.02e-07	0.121
	z=1.5m	9.35e-08	0.111
	Indoor space	9.85e-08	0.117
Condition 4	z=1.2m	9.45e-08	0.112
	z=1.5m	8.60e-08	0.102
	Indoor space	8.96e-08	0.106
Condition 5	z=1.2m	8.43e-08	0.100
	z=1.5m	7.77e-08	0.092
	Indoor space	7.64e-08	0.091
Condition 6	z=1.2m	8.89e-08	0.105
	z=1.5m	8.36e-08	0.099
	Indoor space	8.35e-08	0.099

A comparison of the results shows that the average VOC concentrations for both the planes and the indoor space across all operating conditions are less than 0.60 mg/m³, indicating compliance with the standard.

5. CONCLUSIONS

The following conclusions were drawn in this study:

(a) In terms of the inlet airflow velocity, it was found that, without affecting human comfort, the faster the airflow, the more rapidly the indoor air exchange reached dynamic equilibrium. Furthermore, whether at the breathing plane or within the indoor space, a higher inlet airflow velocity consistently led to a lower average VOC concentration once equilibrium was reached. Therefore, an inlet airflow velocity

of 2.5 m/s can be considered more effective in reducing indoor VOC concentrations.

(b) Under a fixed inlet airflow velocity, the 45° upward airflow provided more thorough disturbance to the indoor air. The area of the "dead zone" generated was smaller, enabling more efficient transport of VOCs to the outdoor environment, thereby reducing indoor VOC concentrations.

(c) Based on the simulation results from the six operating conditions, although all six ventilation methods ultimately achieved indoor VOC concentrations below the national standard, the ventilation method with a 2.5 m/s inlet airflow velocity and 45° upward airflow was found to facilitate faster indoor air exchange for an equilibrium and achieve lower final VOC concentrations compared to other ventilation methods. This, in turn, leads to a reduced potential harm to human health.

(d) Considering all factors, a ventilation method with a larger inlet airflow velocity and an upward inlet airflow angle is recommended, as it can efficiently reduce indoor VOC concentrations, improve indoor air quality, and minimize the harmful effects of pollutants on human health.

ACKNOWLEDGMENT

This paper was supported by Hebei Technological Innovation Center for Volatile Organic Compounds Detection and Treatment in Chemical Industry (Grant No.: ZXJJ20220407).

REFERENCES

[1] GB/T 5206-2015. (2015). Glossary of Terms and Definitions for Paints and Varnishes. https://openstd.samr.gov.cn/bzgk/gb/newGbInfo?hcno=8C006CBE92F6B0758119E6B3C1242963.

[2] Mandin, C., Trantallidi, M., Cattaneo, A., Canha, N., et al. (2017). Assessment of indoor air quality in office buildings across Europe–The OFFICAIR study. Science of the Total Environment, 579: 169-178. https://doi.org/10.1016/j.scitotenv.2016.10.238

[3] Smith, M.T., Zhang, L., McHale, C.M., Skibola, C.F., Rappaport, S.M. (2011). Benzene, the exposome and future investigations of leukemia etiology. Chemico-Biological Interactions, 192(1-2): 155-159. https://doi.org/10.1016/j.cbi.2011.02.010

[4] Khan, H.A. (2007). Benzene's toxicity: A consolidated short review of human and animal studies. Human & Experimental Toxicology, 26(9): 677-685. https://doi.org/10.1177/0960327107083974

[5] Li, L., Li, H., Wang, X.Z., Zhang, X.M., Wen, C. (2013). Pollution characteristics and health risk assessment of volatile organic compounds in the ambient air of Guangzhou's urban centre. Environmental Science, 34(12): 4558-4564. https://www.hjkx.ac.cn/hjkx/ch/reader/view_abstract.aspx?file_no=20131209&flag=1.

[6] The World Health Report. (2002). Geneva: World Health Organization. https://www.who.int/publications/i/item/9241562072.

[7] Huang, K.C., Zhao, Z., Hoag, G.E., Dahmani, A., Block, P.A. (2005). Degradation of volatile organic compounds with thermally activated persulfate oxidation. Chemosphere, 61(4): 551-560. https://doi.org/10.1016/j.chemosphere.2005.02.032

[8] Mamaghani, A.H., Haghighat, F., Lee, C.S. (2017). Photocatalytic oxidation technology for indoor environment air purification: The state-of-the-art. Applied Catalysis B: Environmental, 203: 247-269. https://doi.org/10.1016/j.apcatb.2016.10.037

[9] Zhang, X.Y., Gao, B., Creamer, A.E., Cao, C.C., Li, Y.C. (2017). Adsorption of VOCs onto engineered carbon materials: A review. Journal of Hazardous Materials, 338: 102-123. https://doi.org/10.1016/j.jhazmat.2017.05.013

[10] Hun, D.E., Corsi, R.L., Morandi, M.T., Siegel, J.A. (2010). Formaldehyde in residences: Long-term indoor concentrations and influencing factors. Indoor Air, 20(3): 196-203. https://doi.org/10.1111/j.0905-6947.2010.00644.x

[11] Yang, X., Chen, Q. (2001). A coupled airflow and source/sink model for simulating indoor VOC exposures. Indoor Air, 11(4): 257-269. https://engineering.purdue.edu/~yanchen/paper/2001-11.pdf.

[12] Sun, Z., Huang, Z., Wang, J.S. (2007). Direct numerical simulation of indoor airflow. Journal of Shanghai Jiao Tong University, 41(5): 677-680.

[13] Verniers, K., Losfeld, F., Pollet, I., Laverge, J. (2023). Impact of ventilation type on indoor generated PM and VOC levels for different indoor activities. International Journal of Ventilation, 22(4): 317-326. https://doi.org/10.1080/14733315.2023.2198780

[14] Zemitis, J., Borodinecs, A., Lauberts, A. (2018). Ventilation impact on VOC concentration caused by building materials. Magazine of Civil Engineering, 8(84): 130-139.

[15] Yan, F.Y., Wang, X.H., Wu, Y.C. (2009). CFD-Based Simulation of indoor natural ventilation and thermal comfort. Journal of Tianjin University, 42(5): 407-412.

[16] Lee, H., Awbi, H.B. (2004). Effect of internal partitioning on indoor air quality of rooms with mixing ventilation—Basic study. Building and Environment, 39(2): 127-141. https://doi.org/10.1016/j.buildenv.2003.08.007

[17] Pereira, M.L., Graudenz, G., Tribess, A., Morawska, L. (2009). Determination of particle concentration in the breathing zone for four different types of office ventilation systems. Building and Environment, 44(5): 904-911. https://doi.org/10.1016/j.buildenv.2008.06.006

[18] Visagavel, K., Srinivasan, P.S.S. (2009). Analysis of single side ventilated and cross ventilated rooms by varying the width of the window opening using CFD. Solar Energy, 83(1): 2-5. https://doi.org/10.1016/j.solener.2008.06.004

[19] Cheong, K.W.D., Djunaedy, E., Poh, T.K., Tham, K.W., Sekhar, S.C., Wong, N.H., Ullah, M.B. (2003). Measurements and computations of contaminant's distribution in an office environment. Building and Environment, 38(1): 135-145. https://doi.org/10.1016/S0360-1323(02)00031-8

[20] Ye, W., Won, D.Y., Zhang, X. (2014). A preliminary ventilation rate determination methods study for residential buildings and offices based on VOC emission database. Building and Environment, 79: 168-180. https://doi.org/10.1016/j.buildenv.2014.05.009

[21] Hernandez, G., Wallis, S.L., Graves, I., Narain, S., Birchmore, R., Berry, T.A. (2020). The effect of

ventilation on volatile organic compounds produced by new furnishings in residential buildings. Atmospheric Environment: X, 6: 100069. https://doi.org/10.1016/j.aeaoa.2020.100069
[22] Kang, D.H., Choi, D.H., Seong, Y.B., Yeo, M.S., Kim, K.W. (2013). A numerical simulation of VOC emission and sorption behaviors of adhesive-bonded materials under floor heating condition. Building and Environment, 68: 193-201. https://doi.org/10.1016/j.buildenv.2013.06.013
[23] Xiao, L.Y., Qian, Y.M., Wang, L.W., Wu, Z.M., Meng, W., Hu, Y.M., Ding, C.B., Jing, J.X., Ma, L. (2023). Numerical simulation and experimental study on cyclone adsorption characteristics of volatile organic compounds (VOCs). Chemical Engineering Research and Design, 194: 9-26. https://doi.org/10.1016/j.cherd.2023.04.021
[24] Liu, J., Li, W.Q. (2011). A long-term modelling study of ventilation and VOC distribution in multi-family residential buildings in the severe cold region of China. International Journal of Ventilation, 10(3): 217-226. https://doi.org/10.1080/14733315.2011.11683950
[25] Song, W., Kong, Q.Y., Li, H.M. (2013). Characteristics of VOC mass transfer from wood furniture surface. CIESC Journal, 64(5): 1549-1560. https://doi.org/10.3969/j.issn.0438-1157.2013.05.007
[26] GB/T 18883-2022. (2022). Indoor Air Quality Standards. https://www.hbcdc.cn/jkjy/jkzd/hjyhjws/hjws/kqwryjk/9533.htm.